Biochimica et Biophysica Acta 1837 (2014) 1–13

Contents lists available at ScienceDirect

Biochimica et Biophysica Acta

journal homepage: www.elsevier.com/locate/bbabio

Interactions of subunits Asa2, Asa4 and Asa7 in the peripheral stalk of the mitochondrial ATP synthase of the chlorophycean alga *Polytomella* sp.

Héctor Miranda-Astudillo [a,1], Araceli Cano-Estrada [a,1], Miriam Vázquez-Acevedo [a], Lilia Colina-Tenorio [a], Angela Downie-Velasco [a], Pierre Cardol [b], Claire Remacle [b], Lenin Domínguez-Ramírez [a,2], Diego González-Halphen [a,*]

[a] Instituto de Fisiología Celular, Universidad Nacional Autónoma de México, México D.F., Mexico
[b] Genetics of Microorganisms, Institute of Plant Biology, University of Liège, Liège, Belgium

ARTICLE INFO

Article history:
Received 4 March 2013
Received in revised form 24 July 2013
Accepted 2 August 2013
Available online 9 August 2013

Keywords:
F_1F_O-ATP synthase peripheral-stalk
Dimeric mitochondrial complex V
Chlorophycean algae
Chlamydomonas reinhardtii
Polytomella sp.
Asa subunits

ABSTRACT

Mitochondrial F_1F_O-ATP synthase of chlorophycean algae is a complex partially embedded in the inner mitochondrial membrane that is isolated as a highly stable dimer of 1600 kDa. It comprises 17 polypeptides, nine of which (subunits Asa1 to 9) are not present in classical mitochondrial ATP synthases and appear to be exclusive of the chlorophycean lineage. In particular, subunits Asa2, Asa4 and Asa7 seem to constitute a section of the peripheral stalk of the enzyme. Here, we over-expressed and purified subunits Asa2, Asa4 and Asa7 and the corresponding amino-terminal and carboxy-terminal halves of Asa4 and Asa7 in order to explore their interactions in vitro, using immunochemical techniques, blue native electrophoresis and affinity chromatography. Asa4 and Asa7 interact strongly, mainly through their carboxy-terminal halves. Asa2 interacts with both Asa7 and Asa4, and also with subunit α in the F_1 sector. The three Asa proteins form an Asa2/Asa4/Asa7 subcomplex. The entire Asa7 and the carboxy-terminal half of Asa4 seem to be instrumental in the interaction with Asa2. Based on these results and on computer-generated structural models of the three subunits, we propose a model for the Asa2/Asa4/Asa7 subcomplex and for its disposition in the peripheral stalk of the algal ATP synthase.

1. Introduction

Mitochondrial F_1F_O-ATP synthase (complex V) is the main ATP producing enzyme in non-photosynthetic eukaryotes. The complex works as a rotary motor driven by an electrochemical proton gradient [1,2]. Proton translocation through the Fo sector drives rotation of the central stalk (the gamma subunit) that extends from the membrane-embedded c-ring into the center of the F_1 sector. The conformational changes induced by the gamma subunit in F_1 allow the synthesis of ATP in the catalytic sites of the beta subunits [3]. Chlorophycean algae like *Chlamydomonas reinhardtii* and *Polytomella* sp. exhibit a highly stable, dimeric mitochondrial F_1F_O-ATP synthase with an apparent molecular mass of 1600 kDa [4]. This dimeric complex also has a unique overall architecture exhibiting two stout peripheral stalks as judged by electron microscopy analyses [5–8]. The functional core of the algal enzyme is formed by the eight classic subunits α, β, γ, δ, ε, *a* (ATP6), *c* (ATP9), and OSCP [9]. In addition, the complex contains nine atypical subunits (Asa1 to Asa9) that constitute the robust peripheral stalk and that seem to participate also in the dimerization of the complex [10–13]. The presence of these atypical subunits was originally suggested based on N-terminal sequences of the polypeptide components of the mitochondrial ATP synthase of *C. reinhardtii* [14] and mining of the green algal genome [15]. To date, genes encoding homologs of Asa subunits seem to be present exclusively in chlorophycean algae [13].

The subsequent biochemical characterization of the algal enzyme was carried out with *Polytomella* sp. [7], since this colorless alga, closely related to *C. reinhardtii*, lacks both chloroplasts and cell wall, therefore allowing an easy isolation of mitochondria and purification of its oxidative phosphorylation components [16,17]. Work carried out with the *Polytomella* ATP synthase established neighboring interactions between Asa subunits, mainly through the identification of subcomplexes formed by heat dissociation and by using cross-linking agents [10,12]. In particular, two cross-link products were consistently obtained, with more than one bi-functional reagent: Asa2 + Asa4 and Asa2 + Asa7 [7]. These experiments and others led to the proposal of models of the topological disposition of the Asa polypeptides [7,10,11]. In order to gain more insights on how Asa proteins interact, in this work we over-expressed and purified the recombinant Asa2, Asa4 and Asa7 subunits and explored their interactions in vitro using different experimental

* Corresponding author at: Departamento de Genética Molecular, Instituto de Fisiología Celular, UNAM, Apartado Postal 70-600, Delegación Coyoacán, 04510 México D.F., Mexico. Tel.: +52 55 5622 5620; fax: +52 55 5622 5611.
E-mail address: dhalphen@ifc.unam.mx (D. González-Halphen).
[1] These authors contributed equally to this work.
[2] Present address: Departamento de Ciencias de la Salud, Universidad Autónoma Metropolitana-Lerma, Lerma de Villada, Lerma, Mexico.

0005-2728/$ – see front matter © 2013 Elsevier B.V. All rights reserved.
http://dx.doi.org/10.1016/j.bbabio.2013.08.001

approaches. Based on the obtained data, we propose a refined model for the disposition of these three subunits in the peripheral stalk of the algal, mitochondrial ATP synthase.

2. Materials and methods

2.1. Algal strains and growth conditions

Polytomella spec. (Strain number 198.80, isolated by E.G. Pringsheim) was obtained from the Culture Collection of Algae at the University of Göttingen and grown as previously described [18].

2.2. Polytomella mitochondrial ATP synthase purification

The algal ATP synthase was purified following the described procedure [10].

2.3. Protein analysis

Blue native polyacrylamide gel electrophoresis (BN-PAGE) was carried out as described [19] and denaturing gel electrophoresis was carried out in a Tricine-SDS-PAGE system [20]. When indicated, 1D-BN-PAGE was followed by 2D-Tricine-SDS-PAGE [20]. Protein concentrations were estimated according to Markwell et al. [21].

2.4. Dissociation of the ATP synthase into subcomplexes

The purified algal ATP synthase (120 μg of protein) was incubated for 30 min on ice in the presence of 0.04% lithium dodecyl sulfate (LiDS) and the resulting sample subjected to BN-PAGE in 4–12% gradient acrylamide gels. The lane of interest was excised and incubated in the presence of 1% SDS and 1% β-mercaptoethanol for 15 min and then subjected to 2D Tricine-SDS-PAGE in 14% acrylamide gels.

2.5. Cloning of the cDNAs encoding subunits of the ATP synthase of Polytomella sp. in expression vectors

The cDNAs of *Asa2*, *Asa4-n*, *Asa4-c*, *Asa7*, *Asa7-n*, *Asa7-c* were PCR-amplified from a *Polytomella* sp. cDNA library cloned in λ-ZapII phages using specific oligonucleotide primers: for Asa2, forward 5′-GAC GCT GCC GT(C/G/T) GC(C/G/T) CT(C/T) AC(C/T) TAC-3′ and reverse 5′-TCA (G/A/C)AC (G/A)GC GTA (G/A)CC CTG (G/A/C)GC CTC-3′; for Asa4, forward 5′-GCT ACC GAG CCT GCT GTT TC-3′ and reverse 5′-TTA AGC AGC GAC CTT AGG GC-3′; for Asa4-N, forward 5′-GCT ACC GAG CCT GCT GTT TC-3′ and reverse 5′-TTA CTT GGC CTT AGC CGC AAA-3′; for Asa4-C, forward 5′-AAG TTT GGC CAG GAG ACC-3′ and reverse 5′-TTA AGC AGC GAC CTT AGG GC-3′; for Asa7 forward 5′-CTT ACC ACT TTT ACC TTC-3′ and reverse 5′-CTA TGC TTG GAG AGG AGG AAG-3′; for Asa7-N forward 5′-CTT ACC ACT TTT ACC TTC-3′ and reverse 5′-TTA GTT CTG GAT AGA AGA GTG GAG-3′; for Asa7-C forward 5′-ATC CAG AAC TAC CTC CTT TCT-3′ and reverse 5′-CTA TGC TTG GAG AGG AGG AAG-3′. The resulting amplicons were cloned in a pET28a vector that adds a hexa-histidine tag (6His-tag) in the N-terminus of the corresponding proteins using the following restriction sites: for *Asa2* NheI and SalI; for *Asa4-N* and *Asa4-C*, NdeI and BamHI; and for *Asa7*, *Asa7-N* and *Asa7-C*, NdeI and SalI. The cDNAs of *Asa2, Asa4, Asa4-n, and Asa4-c* were cloned in a pET3a vector (no 6His-tag) using the restriction sites NdeI and BamHI.

2.6. Overexpression of recombinant proteins

All overexpression conditions were similar for the seven proteins. *Escherichia coli* BL21-CodonPlus competent cells were transformed with their corresponding vector by heat shock at 42 °C for 2 min. Bacterial cells were grown in LB medium containing 64 μg/mL chloramphenicol supplemented with 50 μg/mL kanamycin for those expressing the pET28a vector and 100 μg/mL ampicillin for those expressing the pET3a vector. The overexpressed polypeptides were: Asa2 (GenBank GU014474) lacking around 25 residues in the N-terminus and 39 residues in the C-terminus; the complete Asa4 subunit (GenBank GQ168485); the complete Asa7 subunit (GenBank GQ427067), the Asa4-N fragment (16.4 kDa comprising residues 1 to 154 of Asa4), the Asa4-C fragment (14.9 kDa comprising residues 107 to 194 of Asa4), the Asa7-N fragment (7.6 kDa, comprising residues 1 to 77 of Asa7) and the Asa7-C fragment (11.9 kDa, comprising residues 74 to 176 of Asa7).

2.7. Isolation of inclusion bodies

Two liters of culture media was inoculated with bacteria and incubated at 37 °C until an absorbance value of 0.6 at 600 nm was obtained. Then, isopropyl β-D-1-thiogalactopyranoside (IPTG) was added to a 0.1 mM final concentration and the culture was incubated for 16 additional hours. The culture was then centrifuged at 6000 *g* for 15 min, and the resulting pellet resuspended in lysis buffer (50 mM NaH_2PO_4, 500 mM NaCl, 1% Triton X-100, pH 7.8) and sonicated with 8 pulses (setting 5 W, 50% output) of 5 min each using a Branson-450 sonifier. Inclusion bodies (ICBs) were recovered by centrifugation at 12,000 *g* for 10 min. ICBs were then washed as described [22] with slight modifications. ICBs were resuspended in PBS (50 mM NaH_2PO_4, 500 mM NaCl, pH 7.8) containing 5% Triton and immediately after recovered by centrifugation at 12,000 *g* for 10 min. The resulting pellet was resuspended in distilled water and centrifuged in the same conditions. These washes were repeated once again with PBS containing 5% Triton X-100 and three times with distilled water. ICBs were then refrigerated and stored at −80 °C until used.

2.8. Purification of recombinant proteins

All steps were carried out at 4 °C except when indicated. The ICBs were thawed and dissolved in PBS buffer containing 8.0 M urea for 12 h. The solution was centrifuged at 17,500 *g* for 10 min. The recombinant Asa4 polypeptide was dialyzed against 2 L of refolding buffer [30 mM CAPS pH 10.0, 0.5 mM sodium EDTA, 1 mM DTT, and 2% (v/v) glycerol] for 12 h and then centrifuged at 17,500 *g* for 10 min. The resulting supernatant was loaded on a DEAE-Sepharose FF 10/300 column (20 mL) and eluted with a gradient of 0 to 500 mM NaCl in the same refolding buffer. The Asa2, Asa4-N, Asa4-C, Asa7, Asa7-N and Asa7-C proteins were purified in denaturing conditions using affinity chromatography. The samples were diluted with PBS to obtain a final concentration of 4.0 M urea and then, a 1 M imidazole solution in the same buffer was added to reach a final concentration of 10 mM in the sample. Then, the sample was loaded on a 5 mL HisTrap FF crude column (GE Healthcare Life Sciences), equilibrated with PBS containing 4 M urea. The column was washed with the same buffer in the presence of 30 mM imidazole and then, the proteins of interest were eluted with a 30 to 500 mM imidazole gradient. The fractions obtained from the column were analyzed by Tricine-SDS-PAGE, and those enriched with the recombinant protein of interest were collected, mixed, concentrated, and stored at −70 °C until used.

2.9. Antibody production and immunoblotting

Antibodies were generated against subunit Asa4, against the recombinant proteins Asa2 and Asa7-C. Either the entire *Polytomella* ATP synthase (20 to 50 μg of protein per lane) or 20 μg of the recombinant, isolated proteins was resolved by Tricine-SDS-PAGE (14% acrylamide) in the presence of 25 mg/L of Serva Blue G in the upper buffer as described [23]. The ATP synthase Asa4 subunit and the recombinant proteins Asa2 and Asa7-C were excised from the gel, grinded in the presence of 20 mM Tris (pH 7.0), mixed with Freund's complete adjuvant and injected into rabbits for antibody production. Western blot analysis was carried out as described [24] with modifications [25].

Colorimetric detection was carried out using a goat anti-rabbit IgG conjugated with alkaline phosphatase (1:3000 for 2 h) in the presence of nitro-blue tetrazolium chloride and 5-bromo-4-chloro-3′-indolyphosphate p-toluidine salt. The images of the polypeptide bands decorated with the insoluble black-purple precipitates were captured in a HP Scanjet G4050.

2.10. Protein–protein interactions assayed by Far-Western analysis

Far-Western analysis was carried out according to [26]. The isolated ATP synthase of *Polytomella* sp. was subjected to Tricine-SDS-PAGE in 12% acrylamide gels and then transferred to nitrocellulose membranes. The lanes containing the denatured enzyme were incubated in TTBS buffer (20 mM Tris–HCl pH 8.0, 500 mM NaCl, and 0.05% Tween-20), in the presence of increasing concentrations of externally-added, purified Asa2, Asa4, Asa4-N or Asa4-C polypeptides for 4 h. In the case of the Asa7 polypeptide, which tended to aggregate easily, a different buffer was used: 50 mM Tris–HCl pH 8.0, 200 mM sodium EDTA, 2.0 % glycerol, 200 mM NaCl, and 0.5% sodium cholate. The membranes incubated with the externally-added protein were washed 2 times with the corresponding buffer. Then, the antibody against the recombinant protein was added, followed by the secondary antibody, and the membrane stained as described for Western blot analyses [25].

2.11. Protein–protein interactions assayed by affinity chromatography

These experiments were carried out using crude bacterial extracts containing the overexpressed, recombinant subunits Asa7, Asa7-N, Asa7-C and Asa2 (containing a 6His-tag), and the recombinant subunits Asa-4, Asa4-N and Asa4-C (lacking a 6His-tag). ICBs were prepared from 100 mL of bacterial culture, washed and solubilized with 6 M guanidine in PBS buffer (50 mM NaH_2PO_4, 100 mM NaCl, pH 7.8). The insoluble material was removed by centrifugation at 17,500 *g* for 10 min. Each resulting crude extract supernatant containing the corresponding 6His-tagged subunit was loaded onto a 1 mL HisTrap column equilibrated with PBS buffer. Then the column was washed with PBS containing 30 mM imidazole, 0.01% Tween-20 and 3 M guanidine, followed by a second wash with the same buffer in the presence of 1 M guanidine and a third and final wash with the same buffer containing 0.5 M guanidine. Also, 0.01% of Tween-20 was added to the supernatants containing the recombinant proteins lacking a 6His-tag, followed by dialysis against PBS buffer. Each dialyzed crude extract sample was loaded onto the HisTrap column where one of the proteins with 6His-tag was previously bound. The columns were washed with PBS buffer containing 0.01% Tween-20 and 30 mM imidazole. Then, an imidazole gradient from 30 to 500 mM was applied in order to elute the proteins that remained bound to the column. Whenever the 6His-tagged protein coeluted with the non 6His-tagged protein, both proteins were considered to have interacted inside the column. The absorbance at 280 nm of the eluted fractions was monitored and selected fractions were subjected to Tricine-SDS-PAGE (12% acrylamide) and then transferred to a nitrocellulose membrane. Proteins were analyzed by Western blot using specific antibodies.

In order to assess any possible unspecific binding the recombinant subunit of interest, lacking a 6His-tag, was loaded onto a 1 mL HisTrap column with no bound protein.

2.12. Protein–protein interactions assayed by Blue Native Electrophoresis

One nanomole of each subunit was mixed in a denaturing solution containing 50 mM Bis–Tris pH 7.0, 4 mM DTT, 750 mM ε-amino caproic acid, 0.15% SDS and 0.1% Coomassie Brilliant Blue G. The mixture was incubated at 94 °C during 10 min and subjected to BN-PAGE in 12% acrylamide gels [20] at 4 °C. Proteins were expected to renature in the BN-gel and establish specific interactions. Gels were run at 80 V for 1.5 h and then at 200 V, until the desired separation of polypeptides was achieved. For interaction assays in the presence of Asa7, gels containing 14% acrylamide were used. Selected lanes of the BN-gels were then subjected to 2D-Tricine-SDS-PAGE.

2.13. Protein stability at different pHs

Samples containing two nanomoles of the proteins of interest or the mixture of two proteins, were dialyzed at 4 °C against 500 mM NaCl and 20 mM of each one of the following buffers: phosphates (pH 2.0), acetate (pH 4.0), Mes (pH 6.0), MOPS (pH 7.0), Tris (pH 8.0) or CAPS (pH 10.0). Then, samples were centrifuged at 17,500 *g* and both the pellet and a fraction of the supernatant were analyzed by Tricine-SDS-PAGE.

2.14. Formation of an Asa2/Asa4/Asa7 subcomplex

All steps were performed at 4 °C unless otherwise stated. The Asa4 subunit was purified as described in Section 2.8 except that 0.01% Tween 20 was added to the buffer. The enriched fractions identified by Tricine-SDS-PAGE were mixed and stored at −70 °C until used. The 6His-tagged Asa7 subunit was purified as mentioned in Section 2.8 except that three HisTrap FF columns (GE Healthcare Life Sciences) joined in tandem were used and 0.05% Tween 20 was added to the buffer. The enriched fractions were mixed and concentrated up to 0.4 mg/mL in an Amicon Ultra-15 centrifugal filter unit (Millipore). For Asa2 subunit, the sample of solubilized ICBs obtained as described in Section 2.8 was diluted to 400 mL with a buffer containing 30 mM CAPS, 0.5 mM EDTA, 0.5 mM DTT, 2% glycerol pH 10.0 and then loaded onto a DEAE Sepharose FF 10/300 column (20 mL) equilibrated with the same buffer. The protein was eluted with a linear NaCl gradient from 0 to 500 mM in the same buffer (10 column volumes). The eluted fractions were analyzed in Tricine-SDS-PAGE and the enriched fractions were mixed and stored at −70 °C until used.

Purified Asa4 (untagged) and Asa7 (6His-tagged) subunits (10 mg of each protein) were mixed and dialyzed together against 3 L of a buffer containing 50 mM NaH_2PO_4, 500 mM NaCl, 0.05% and Tween 20 pH 7.8 for 12 h. The sample was centrifuged at 17,500 *g* for 10 min, imidazole was added to a final concentration of 30 mM, and 750 μL of Ni Sepharose 6 FF resin (Amersham Biosciences) was added to the mixture. The sample was incubated under continuous shaking for 8 h and then washed ten times by centrifugation at 500 *g* for 5 min with 7 mL of the same buffer containing imidazole 30 mM. The Asa4/Asa7 subcomplex was recovered with two 7 mL volumes containing 500 mM imidazole in the same buffer.

The purified Asa4/Asa7 subcomplex was mixed with 38 mg of purified Asa2 subunit (untagged) and dialyzed against 3 L of a buffer containing 50 mM NaH_2PO_4, 200 mM NaCl, 0.05% Tween 20 pH 7.8 and incubated under continuous shaking for 8 h. The sample was then centrifuged at 17,500 *g* for 10 min, loaded on a 1 mL HisTrap FF column (GE Healthcare Life Sciences) and recirculated for 8 h using a LKB-Peristaltic-Pump P-1 (Pharmacia) at a flow of 0.5 mL min^{-1}. Then, the column was attached to an ÄKTA monitor UPC-900 Workstation (GE Healthcare Life Sciences) washed with the same buffer containing 30 mM imidazole until a base line was obtained (30 column volumes) and the subcomplex was eluted when a linear imidazole gradient from 30 to 500 mM was applied. The eluted fractions were analyzed by Tricine-SDS-PAGE to identify those that corresponded to the Asa2/Asa4/Asa7 subcomplex.

2.15. Stoichiometry of subunits in the Asa2/Asa4/Asa7 subcomplex

Purified ATP synthase from *Polytomella* sp. and the isolated, recombinant ASA7 subunit (6His-tagged) were separated in a Tricine-SDS-PAGE at increasing known protein concentrations. The resulting gels were stained with Coomassie Blue. Gel images were captured in a Gel-ChemiDoc Scanner System (Bio-Rad) and the densitometric analysis was performed with the program GelAnalyzer 2010a (http://www.

gelanalyzer.com/index.html). A graph of peak area of the polypeptide bands versus protein quantities (in picomoles) was constructed and adjusted to a linear function. Each fraction corresponding to the obtained Asa2/Asa4/Asa7 subcomplex elution was also separated in a Tricine-SDS-PAGE and the densitometry data from each band was interpolated to the corresponding linear function obtained from the Asa2 and Asa4 subunits of the ATPase and from the recombinant, isolated 6His-tagged Asa7 protein. Thus, we estimated the stoichiometry of subunits Asa2:Asa4:Asa7 in the Asa2/Asa4/Asa7 subcomplex.

2.16. Protein structure prediction and protein–protein docking

Isoelectric points were calculated using "Compute pI/Mw" at EXPASY (http://web.expasy.org/cgi-bin/compute_pi/pi_tool). The model of subunits Asa2 (lacking the first 7 residues of the N-terminal region and the last 43 residues of the C-terminal region) and the full-length Asa4 were made in Robetta server (http://robetta.bakerlab.org) of the University of Washington [27]. In both cases, a set of 5 possible models was obtained. The model of subunit Asa7 was made with the Quark program at the Zhang Lab server of the University of Michigan (http://zhanglab.ccmb.umich.edu/Quark/) [28]. A set of ten possible models were obtained. The model number 2 of every subunit was chosen because of its solvent exposed residues and because it exhibited an elongated structure, as expected of a component of the peripheral stalk. Hydrogen atoms and charges were added to the Asa2, Asa4 y Asa7 models and 1000 steps (steepest descent set at 0.02 Å per step) of energy minimization were carried out using the ff99SB forcefield of UCSF Chimera software (http://www.cgl.ucsf.edu/chimera/) [29]. Protein–protein docking prediction was carried out in the Vakser Lab server of the University of Kansas (http://Vakser.bioinformatics.Ku.edu/resources/gramm/grammx/) [30]. The docking prediction between Asa4 and Asa7 subunits was carried out first. A set of 50 possible models were obtained. All the models that did not exhibit an interaction in accordance with the data obtained in this work were discarded. The model that predicted an interaction between the carboxy-terminal half of Asa4 and the carboxy-terminal half of Asa7 was selected. The in silico Asa4/Asa7 subcomplex was then used to dock the Asa2 subunit. A new set of 50 possible models were obtained, where the final model was chosen in accordance with the obtained experimental results. The interfaces of the subcomplex obtained were analyzed by Dimplot [31] and the surface calculations for cavities as implemented in PyMol (http://www.pymol.org/, The PyMOL Molecular Graphics System, Version 1.5.0.4 Schrödinger, LLC) in order to assess their packing quality.

3. Results

3.1. Over-expression and purification of recombinant Asa subunits

In order to address the study of the interaction of some of the subunits that constitute the peripheral stalk of the ATP synthase of *Polytomella* sp., the corresponding polypeptides were over-expressed and purified as described in Sections 2.6, 2.7 and 2.8, and compared to the polypeptide pattern of the isolated ATP synthase. The purified recombinant subunits Asa2, Asa4 and Asa7, and their corresponding fragments Asa4-N, Asa4-C, Asa7-N and Asa7-C were loaded on a Tricine-SDS-gel (Fig. 1). All recombinant subunits exhibit a single, main polypeptide, although discrete bands that may represent dimeric forms were observed in some preparations (Fig. 1, lanes 4 and 5). Antibodies raised against subunits Asa2, Asa4 and Asa7 of the *Polytomella* ATP synthase also recognized the corresponding purified recombinant subunits, and the anti-Asa4 antibody recognized the Asa4-N and Asa4-C fragments, albeit the Asa4-N fragment more poorly (Suppl. Fig. 1). This suggests that the main immunogenic epitopes of Asa4 are found in its carboxy-terminal region.

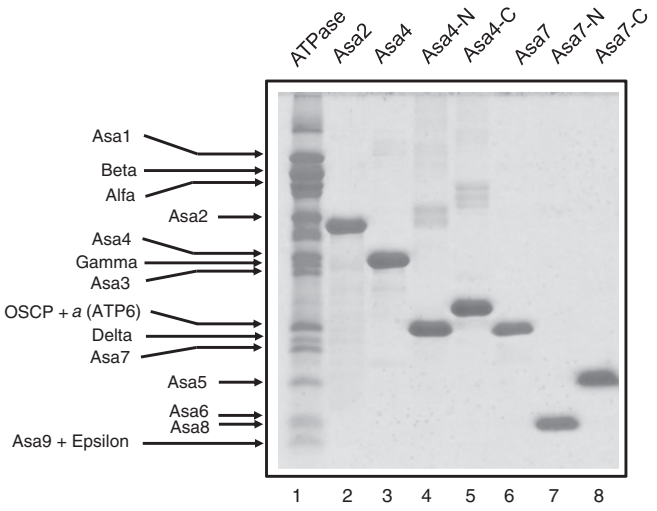

Fig. 1. *Polytomella* ATP synthase and the recombinant Asa subunits used in this work. Tricine-SDS polyacrylamide gel showing the polypeptide pattern of the *Polytomella* ATP synthase complex (25 μg of protein, lane 1). The identity of its 16 subunits is indicated. Three micrograms of each recombinant Asa subunits overexpressed and purified in this work was loaded in lanes 2 to 8. Some of the recombinant proteins, like Asa7, exhibit slightly higher apparent molecular masses than the original subunits due to the presence of the 6His-tag. In contrast, Asa2 exhibits a lower molecular mass, due to the absence of several residues in its N- and C-termini. Molecular masses are 38.6 kDa for Asa2 (lane 2), 31.2 kDa for Asa4 (lane 3), 16.4 kDa for Asa4-N (lane 4), 14.9 kDa for Asa4-C (lane 5), 20.5 kDa for Asa7 (lane 6), 7.6 kDa for ASA7-N (lane 7), and 11.9 kDa for Asa7-C (lane 8).

3.2. On the interaction of Asa4 and Asa7

Far-Western blotting is one of the techniques employed to detect protein–protein interactions. We first assayed a possible interaction between the purified, recombinant Asa4 subunit and the entire ATP synthase, exploring the possibility that the recombinant polypeptide could bind to some of the subunits of the complex. Several lanes of nitrocellulose membrane containing the same concentration of ATP synthase were incubated with increasing concentrations of the isolated, recombinant Asa4 subunit and then decorated with the anti-Asa4 antibody mentioned above (Fig. 2A). As expected, the anti-Asa4 antibody strongly recognized the original Asa4 polypeptide of the ATP synthase in all lanes. Nevertheless, at increasing concentrations of the externally added, recombinant Asa4, the antibody started to recognize a second band, which was identified as Asa7, based on its molecular mass (Fig. 2A, lanes 4 to 7). This indicated that the externally added, recombinant Asa4 subunit interacted with the Asa7 polypeptide bound to the nitrocellulose membrane, and was therefore also recognized by the

Fig. 2. Interaction of Asa4 with Asa7. A, B) Far-Western analyses of *Polytomella* ATP synthase (25 μg of protein per lane) incubated for 4 h with increasing nanomoles of the isolated, recombinant Asa4 (A) and Asa7 (B) polypeptides as indicated (in a 5 mL final volume), and then decorated with an anti-Asa4 (A) or an anti-Asa7 (B) antibody. C) Interaction of Asa4 and Asa7 assayed by affinity chromatography. The crude extract containing expressed Asa4 subunit was loaded on a 1 mL HisTrap column containing no bound protein (upper panel) or to which the Asa7 subunit, containing a 6His-tag, was previously bound (lower panel). Western blot decorated with anti-Asa4 and anti-Asa7 antibodies of the fractions eluted from the column upon application of a 30 to 500 mM imidazole gradient. Lane 1, crude extract loaded on the column; lane 2, protein excluded from the column; lanes 3 and 4, proteins excluded from the column after washing with 30 mM imidazole. D) Identification of Asa4–Asa7 subcomplexes. One nanomole of each protein was incubated together in a final volume of 50 μL and loaded onto 1D-BN-PAGE followed by 2D-Tricine-SDS-PAGE. A putative Asa4–Asa7 subcomplex is indicated with a white arrow. Three micrograms of each of the molecular mass markers, Asa4 (31.2 kDa), Asa4-C (14.9 kDa) and Asa7 (20.5 kDa) was loaded on the gel on its left-hand side. E) Stability of the isolated, recombinant Asa4 and Asa7 subunits at different pHs. Two nanomoles of Asa4 (upper panel), Asa7 (middle panel) and a mixture of Asa4 and Asa7 (lower panel) in 100 μL final volume were dialyzed against buffers with the indicated pHs and centrifuged. Then, 30 μL of each pellet and supernatant was loaded on the gel.

anti-Asa4 antibody. At relatively high concentrations of externally-added Asa4, the anti-Asa4 antibody also recognized Asa1 (Fig. 2A, lanes 6 and 7). We interpret this signal as a weak interaction of Asa4 with Asa1. In all the Far-Western experiments, the bands that appeared at high concentration of the recombinant, isolated protein were interpreted with caution, since unspecific interactions may occur.

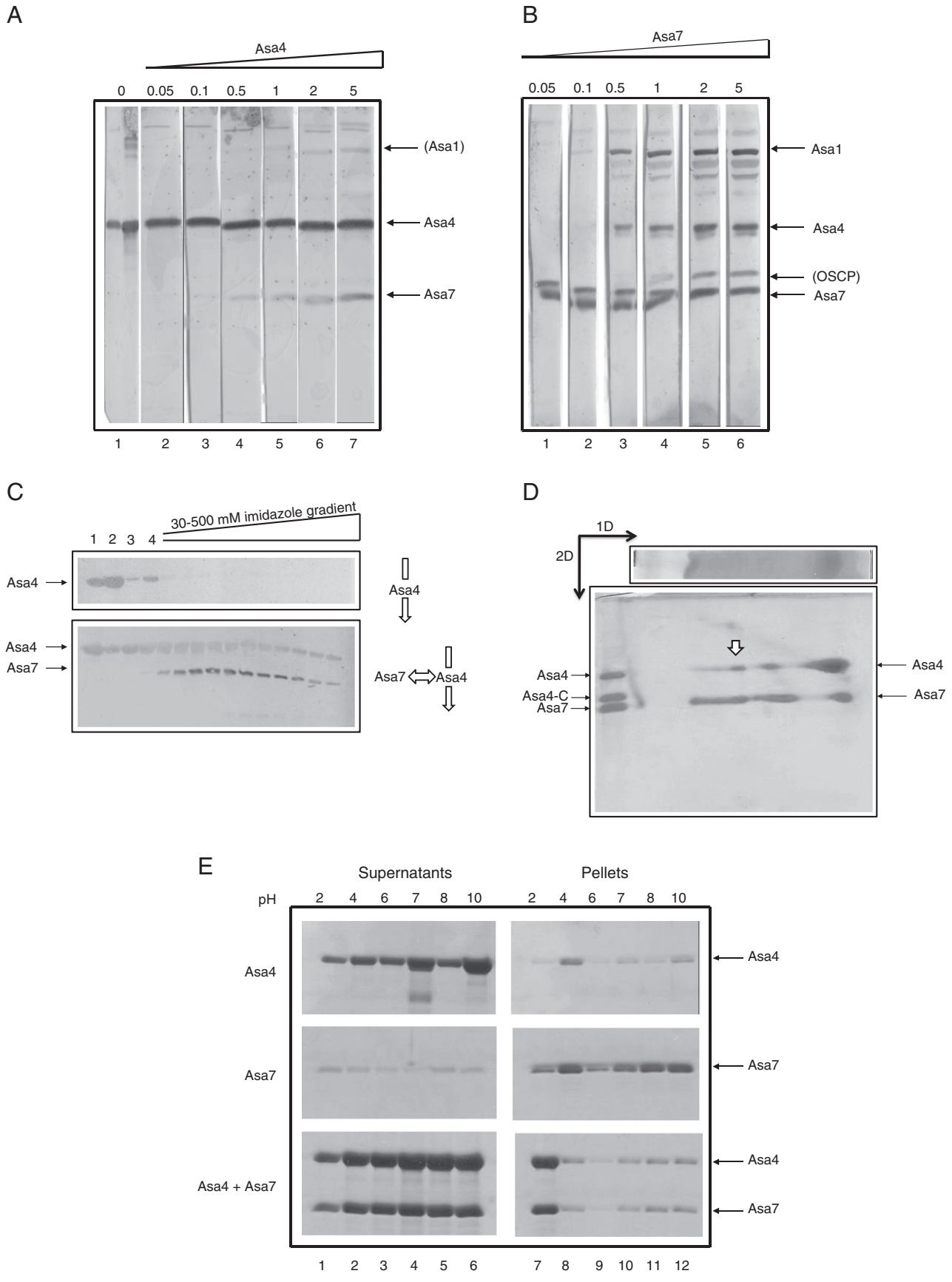

We predicted that the complementary Far-Western experiment, now using the isolated, recombinant Asa7, should recognize the original Asa4 subunit of the ATP synthase complex. Lanes containing the same concentration of ATP synthase were incubated with increasing concentrations of the isolated, recombinant Asa7 subunit and decorated with an anti-Asa7 antibody (Fig. 2B). As expected, the anti-Asa7 antibody recognized the Asa7 subunit of ATP synthase in all lanes. At increasing concentrations of externally-added recombinant Asa7, the antibody also recognized additional bands, corresponding to Asa1, Asa4 and OSCP (Fig. 2B, lanes 3 to 6). This suggested that Asa7 may interact with these three subunits.

In order to further explore the interaction of Asa4 and Asa7 with a different experimental approach, the isolated, recombinant Asa7 containing a 6His-tag, was bound to a HisTrap nickel column. Then, the recombinant Asa4 (lacking a 6His-tag) was loaded on the column and washed with 30 mM imidazole. A second identical column, containing only the nickel matrix with no protein bound to it, was loaded with Asa4 (lacking the 6His-tag) and run in parallel. This second column served as a control to assay a possible adventitious interaction of Asa4 with the nickel matrix. While Asa4 readily eluted in the first fractions of the column lacking bound Asa7 (Fig. 2C, upper panel), Asa4 was retained in the column containing the 6His-tagged Asa7. In order to recover both proteins, the column was eluted in the presence of a 30 to 500 mM imidazole gradient, that released Asa7 along with its bound Asa4 (Fig. 2C, lower panel).

The interaction of Asa4 and Asa7 was also assayed using an additional approach. A mixture of isolated, denatured, recombinant Asa4 and Asa7 was subjected to BN-PAGE, expecting that during the non-denaturing electrophoretic technique both proteins would renature and interact, forming an Asa4/Asa7 subcomplex. To analyze these non-denaturing gels, the lanes obtained from BN-PAGE were subjected to 2D-Tricine-SDS-PAGE. Although a large amount of free Asa4 and Asa7 migrated to the front of the 1D-BN gel, discrete bands with a higher molecular mass were observed, suggesting the formation of an Asa4/Asa7 subcomplex (Fig. 2D, bands indicated with a white arrow).

The interaction of Asa4 and Asa7 was finally explored using a fourth different technique. The stability of the two isolated, recombinant Asa4 and Asa7 proteins was assayed by incubation at different pHs followed by centrifugation. If the protein was not soluble at a certain pH, it would precipitate and would be recovered in the corresponding pellet after centrifugation. Asa4 (pI = 5.19) was highly soluble, since it was recovered in the supernatants at almost all the pHs explored (from 2.0 to 10.0), while only small amounts precipitated at pH 4.0 and 10.0 (Fig. 2E, upper panels). In contrast, Asa7 (pI = 9.03) was less soluble, and tended to precipitate easily, so it was mainly recovered in the pellets (Fig. 2E, middle panels). A mixture of Asa4 and Asa7 recombinant proteins was also incubated at different pHs and then subjected to differential centrifugation. When Asa7 was in the presence of Asa4, both proteins remained in the soluble fraction, except at pH 2.0, where they both partially precipitated (Fig. 2E, lower panels). Thus, these experiments suggest that Asa4 tends to stabilize Asa7 and maintain it in solution, probably preventing its aggregation by protein–protein interactions.

3.3. On the interaction of Asa4 fragments and Asa7

In order to determine which domains of Asa4 and Asa7 are critical for interaction, lanes containing the same concentration of ATP synthase were transferred to a nitrocellulose membrane and incubated with increasing concentrations of the recombinant Asa4-C fragment. Then, the membranes were decorated with the anti-Asa4 antibody (Fig. 3A). As in previous experiments, the anti-Asa4 antibody recognized the Asa4 subunit of ATP synthase in all lanes. Nevertheless, at increasing concentrations of externally-added Asa4-C fragment, the antibody recognized additional bands, corresponding to Asa1 and Asa7, and more faintly, OSCP (Fig. 3A, lanes 3 to 5). This indicated that the externally added recombinant Asa4-C fragment may interact with these subunits. In contrast, when the same experiment was carried out with the Asa4-N fragment, the anti-Asa4 gave a much weaker signal on subunits Asa1, OSCP and Asa7 (Suppl. Fig. 2). We conclude that Asa4-N interacts loosely with these subunits, although the low signals observed may also be due to the poor recognition of the Asa4-N fragment by the anti-Asa4 antibody (Suppl. Fig. 1, lane 3).

In order to further assess the interaction of Asa4-N and Asa4-C with Asa7, the isolated, recombinant Asa7 containing a 6His-tag, was bound to a nickel column. Then, the recombinant Asa4-N (lacking the 6His-tag) was loaded into the column and washed with 30 mM imidazole. As expected, Asa4-N did not bind to the nickel control column lacking Asa7 (Suppl. Fig. 3, upper panel). Asa4-N also did not bind to the column to which Asa7 was attached (Suppl. Fig. 3, lower panel). This suggests a poor interaction of the Asa4-N fragment with Asa7. In contrast, when Asa4-C was loaded into a column containing Asa7, it was readily retained. Subsequently, in the presence of a 30–500 mM imidazole gradient, Asa4-C and Asa7 co-eluted (Fig. 3B). Since Asa4-C and Asa7 have a similar molecular mass, and therefore migrate together in Tricine-SDS-PAGE, separate Western blot analyses of the column fractions were carried out in order to follow the fate of each protein. Fractions from the column containing Asa4-C were decorated with an anti-Asa4 antibody (Fig. 3B, middle panel), while another aliquot of the same fractions was used to decorate Asa7 elution pattern with an anti-Asa7 antibody (Fig. 3B, lower panel). Some of the Asa7 subunit was partially degraded in the column (the degradation products are indicated by an asterisk in Fig. 3B). The obtained results led us to conclude that Asa4-C interacts with Asa7.

In order to assay the possible formation of a subcomplex between Asa4-C and Asa7, a mixture of the isolated, recombinant Asa4-C and Asa7 proteins was subjected to BN-PAGE followed by 2D-Tricine-SDS-PAGE. Besides the free Asa4-C and Asa7 subunits that migrated to the front of the 1D-BN gel, higher molecular mass bands indicating the presence of an Asa4-C/Asa7 subcomplex were observed (Fig. 3C, lower panel). In contrast, only a small amount of an Asa4-N/Asa7 subcomplex was present when the mixture of Asa4-N and Asa7 was subjected to BN-PAGE and 2D-Tricine-SDS-PAGE, suggesting a more loose interaction of these proteins (Fig. 3C, upper panel).

3.4. On the interaction of Asa7 fragments and Asa4

Two protein fragments of Asa7 were also overexpressed, Asa7-N and Asa7-C (the N-terminal and C-terminal halves of Asa7 respectively). To explore the interaction of Asa7 fragments with Asa4, the isolated, recombinant Asa7 fragments, containing a 6His-tag, were independently bound to nickel columns. Then, the recombinant Asa4 (lacking the 6His-tag) was loaded to the columns and washed with 30 mM imidazole. Asa4 did not bind to the nickel column containing Asa7-N (Suppl. Fig. 4) but it was retained in the column to which Asa7-C was attached (Fig. 4A). Furthermore, the interactions of Asa7 fragments with Asa4 fragments were also explored. Both recombinant Asa7-N and Asa7-C were independently bound to nickel columns. The recombinant Asa4-N fragment (lacking the 6His-tag) was loaded to the column containing Asa7-N and washed with 30 mM imidazole. All the Asa4-N eluted from the column, suggesting a poor interaction of Asa4-N with Asa7-N (Suppl. Fig. 5). In contrast, when Asa4-C was loaded to the column that contained bound Asa7-C, the fragment was retained in the column, and when a 30 to 500 mM imidazole gradient was applied, both proteins were recovered (Fig. 4B).

A mixture of isolated, recombinant Asa4 and the Asa7-N and Asa7-C fragments was also subjected to BN-PAGE followed by 2D-Tricine-SDS-PAGE. The resulting electrophoretic pattern of Asa4 and Asa7-N yielded no subcomplex that would suggest an interaction between these polypeptides (Fig. 4C, upper panel). In contrast, the formation of an Asa4/Asa7-C subcomplex was observed in the corresponding 2D-Tricine-SDS-PAGE polypeptide pattern (Fig. 4C, lower panel, white arrow).

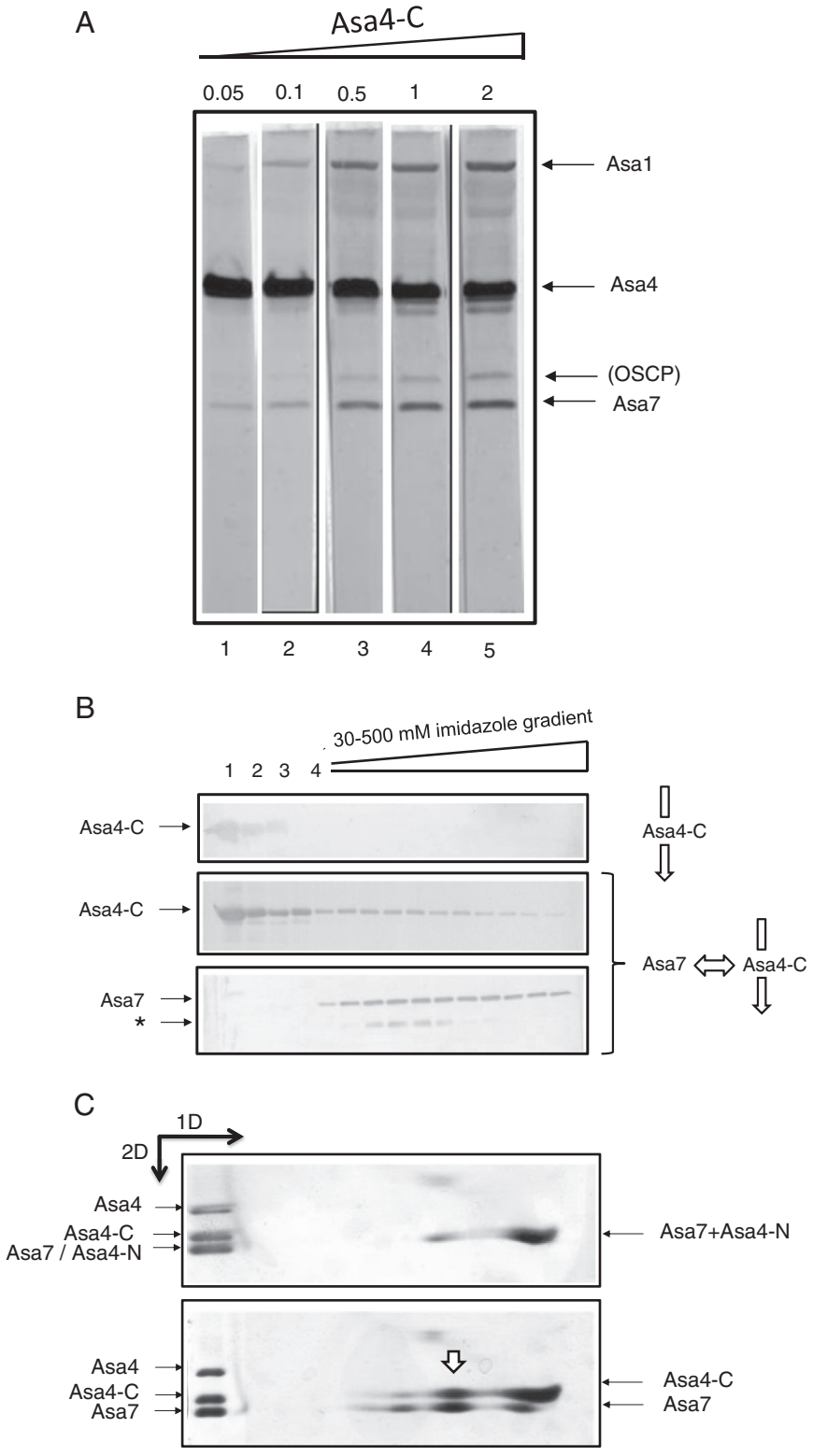

Fig. 3. Interaction of Asa4 fragments with Asa7. A) Far-Western analysis of *Polytomella* ATP synthase (25 μg of protein per lane) incubated for 4 h with increasing nanomoles of the isolated, recombinant Asa4-C fragment as indicated (in a 5 mL final volume), and then decorated with an anti-Asa4 antibody. B) Interaction of the Asa4-C fragment and Asa7 assayed by affinity chromatography. The crude extract containing the expressed Asa4-C fragment was loaded on a 1 mL HisTrap column containing no bound proteins (upper panel) or to which the Asa7 subunit, containing a 6His-tag, was previously bound (middle and lower panels). Western blot decorated with anti-Asa7 (lower panel) or anti-Asa4 (upper and middle panels) of the column fractions collected upon application of a 30 to 500 mM imidazole gradient. Lane 1, crude extract loaded on the column; lane 2, protein excluded from the column; lanes 3 and 4, proteins excluded from the column after washing with 30 mM imidazole. C) Identification of subcomplexes Asa4-N/Asa7 and Asa4-C/Asa7. One nanomole of each polypeptide was incubated together in a final volume of 50 μL and loaded onto 1D-BN-PAGE followed by 2D-Tricine-SDS-PAGE. Upper panel: a small amount of Asa7–Asa4-N subcomplex was formed in these conditions. Lower panel: A putative Asa4-C/Asa7 subcomplex is indicated with a white arrow. Three micrograms of each of the molecular mass markers, Asa4 (31.2 kDa), Asa4-C (14.9 kDa) and Asa7 (20.5 kDa) was loaded on the left-hand side of the gels.

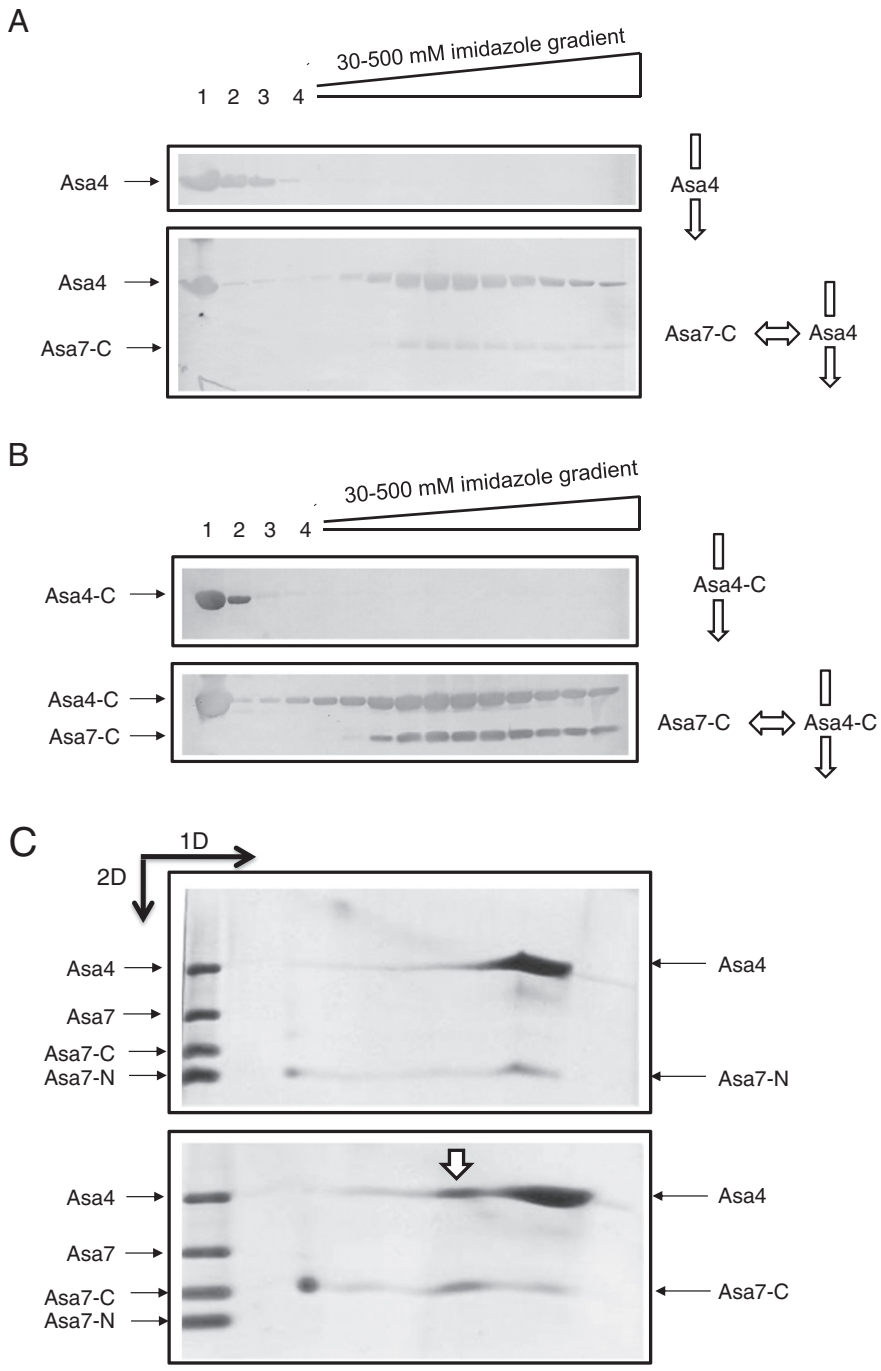

Fig. 4. Interaction of Asa4 with Asa7 fragments. A, B) Interaction of Asa4 and the Asa7 fragments assayed by affinity chromatography. The crude extract containing the recombinant Asa4 subunit (A) or Asa4-C fragment (B) was loaded on a 1 mL HisTrap column containing no bound protein (upper panel) or to which the Asa7-C fragment, containing a 6His-tag, was previously bound (lower panel). Western blot decorated with both an anti-Asa4 and an anti-Asa7 antibody of the column fractions collected upon application of a 30 to 500 mM imidazole gradient. Lane 1, crude extract loaded on the column; lane 2, protein excluded from the column; lanes 3 and 4, proteins excluded from the column after washing with 30 mM imidazole. C) Identification of an Asa4/Asa7-C subcomplex (lower panel). One nanomole of each polypeptide was incubated together in a final volume of 50 μL and loaded onto 1D-BN-PAGE followed by 2D-Tricine-SDS-PAGE. A putative Asa4/Asa7-C subcomplex is indicated with a white arrow. Three micrograms of each of the molecular mass markers, Asa4 (31.2 kDa), Asa7 (20.5 kDa), Asa7-C (11.9 kDa) and Asa7-N (7.6 kDa) was loaded on the gel on its left-hand side. Same experiment conducted with Asa4 and the Asa7-N fragment (upper panel).

Altogether, the data strongly suggest that Asa7 and ASA4 interact through their C-terminal halves.

3.5. On the interaction of Asa2 and Asa4

We also explored the interaction of Asa2 with Asa4 by Far-Western blot analysis. For this purpose, several lanes containing equivalent amounts of ATP synthase were incubated in the presence of increasing concentrations of the recombinant Asa2 polypeptide and decorated with an anti-Asa2 antibody (Fig. 5A). As expected, the anti-Asa2 recognized the natural Asa2 polypeptide in all lanes, but at increasing concentrations of Asa2 the antibody recognized additional bands, mainly Asa1 and Asa4, and more faintly, OSCP and Asa7 (Fig. 5A). This result suggests the interaction of Asa2 with all the four above-mentioned subunits. It is important to note, however, that while externally-added Asa2 seems to recognize subunits Asa4 and Asa7 embedded in the nitrocellulose membrane, neither the externally-added Asa4 nor Asa7 recognized the Asa2 subunit blotted on the membrane (Fig. 2A and 2B).

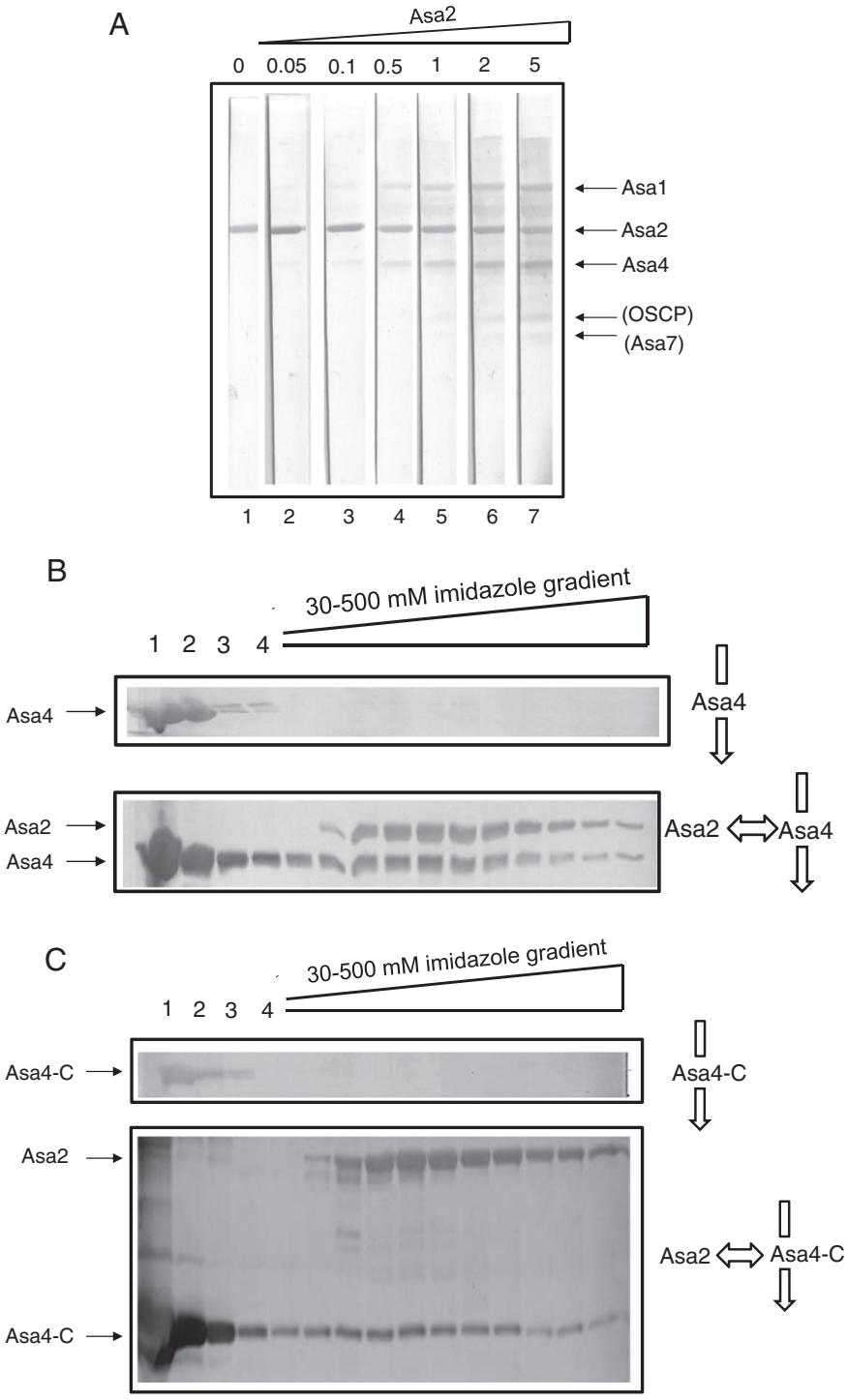

Fig. 5. Interaction of Asa2 with Asa4 and its Asa4-C fragment. A) Far-Western analysis of *Polytomella* ATP synthase (25 μg of protein per lane) incubated for 4 h with increasing nanomoles of the isolated, recombinant Asa2 protein as indicated (in a 5 mL final volume), and then decorated with an anti-Asa2 antibody. B, C) Interaction of Asa4 with Asa2 assayed by affinity chromatography. The crude extract containing the recombinant Asa4 subunit (B) or the Asa4-C fragment (C) was loaded on a 1 mL HisTrap column containing no bound proteins (upper panels) or to which Asa2, containing a 6His-tag, was previously bound (lower panels). Western blot decorated with both anti-Asa2 and anti-Asa4 antibodies of the column fractions collected upon application of a 30 to 500 mM imidazole gradient. Lane 1, crude extract loaded on the column; lane 2, protein excluded from the column; lanes 3 and 4, proteins excluded from the column after washing with 30 mM imidazole.

In order to assess the interaction of Asa2 with Asa4 using an alternative method, the isolated, recombinant Asa2 containing a 6His-tag, was bound to a nickel column. Then, the recombinant Asa4 subunit (lacking the 6His-tag) was loaded to the column and washed with 30 mM imidazole. Asa4 was readily retained by the Asa2 containing column, and both proteins co-eluted in the presence of a 30 to 500 mM imidazole gradient (Fig. 5B). In contrast, the Asa4-N fragment was not retained by the column containing Asa2 (Suppl. Fig. 6). When the Asa4-C fragment was loaded onto the column containing Asa2, it was also readily retained (Fig. 5C), and both proteins co-eluted in the presence of the imidazole gradient. Altogether, the data suggest that Asa2 interacts with Asa4 mainly through the C-terminal half of Asa4.

3.6. On the interaction of Asa2 and Asa7

To explore the interaction of Asa2 and Asa7, the isolated, recombinant Asa7 containing a 6His-tag, was bound to a nickel column. Then, the recombinant Asa2 (lacking the 6His-tag) was loaded on the column and washed. Asa2 was readily retained by the Asa7 containing column, and both proteins co-eluted in the presence of the imidazole gradient (Fig. 6). In this experiment, some degradation products were also observed (see asterisks).

In order to assess which portion of the Asa7 subunit interacts with Asa2, Asa7-N containing a 6His-tag was now bound to a HisTrap nickel column and subsequently Asa2 (lacking the 6His-tag) was loaded. Asa2 was retained in the column to which Asa7-N was attached (Suppl. Fig. 7A). Both Asa2 and Asa7-N polypeptides were recovered upon elution with a 30–500 mM imidazole gradient, nevertheless Asa2 seems to elute before Asa7-N. Elution of a 6His-tagged protein at different concentrations of imidazole suggests the presence of distinct monomeric and oligomeric forms, with multiple 6His-tags on an oligomer. Thus, the Asa7-N fragment could have strongly self-dimerized and so eluted only at higher imidazole concentrations. A similar effect was observed when Asa2 was loaded onto a column with the Asa7-C fragment bound to the nickel matrix. Asa2 was retained in the column to which Asa7-C was attached (Suppl. Fig. 7B), and both proteins were recovered when the imidazole gradient was applied to the column. The data suggest that both halves of the Asa7 subunit (Asa7-N and Asa7-C) seem to be important in the interaction of Asa2 and Asa7.

3.7. Subunits Asa2, Asa4 and Asa7 associate to form a stable subcomplex

In order to corroborate the interactions described above, we reconstituted a subcomplex containing the three recombinant subunits. The isolated recombinant Asa4 (untagged) and Asa7 (6His-tagged) subunits were dialyzed together and co-purified in batch by affinity chromatography. The presence of the Asa4 subunit allows the proper refolding and interaction with the subunit Asa7 as described above (Fig. 2E, Lower panel). The purified Asa4/Asa7 subcomplex was incubated with the isolated Asa2 subunit (untagged). The reconstituted Asa2/Asa4/Asa7 subcomplex was purified by affinity chromatography in column and the three subunits co-eluted with a linear imidazole gradient. The obtained fractions were subjected to Tricine-SDS-PAGE, and the Coomassie Blue-stained showed the presence of excess free Asa4 subunit in the wash fractions of the column and the presence of the three subunits in a stable complex (Fig. 7). The Coomassie Blue-stained bands were analyzed by densitometry and compared to those of the complete *Polytomella* sp. ATP synthase (Asa2 and Asa4) and isolated ASA7 subunit. We conclude that the isolated, recombinant Asa2, Asa4 and Asa7 subunits may interact to form a stable subcomplex with a 1:1:1 stoichiometry. This is in accordance with an earlier proposal that all Asa subunits may have a 1:1 stoichiometry relative to the gamma subunit [7].

3.8. Generation of subcomplexes of the mitochondrial ATP synthase of Polytomella sp. by detergent treatment

Partial dissociation of the ATP synthase by different methods generates subcomplexes which are assumed to keep the original subunit–subunit interactions that exist in the intact enzyme [7]. Here, the *Polytomella* sp. ATP synthase was dissociated in ice in the presence of 0.04% LiDS and subjected to BN-PAGE followed by Tricine-SDS-PAGE. A 100 kDa subcomplex formed by ASA2 and subunit alfa was observed (Fig. 8), suggesting the close proximity of ASA2 to the F_1 catalytic sector of the enzyme.

3.9. Model for the interaction between subunits Asa2, Asa4 and Asa7

We integrated the results obtained in this work in the model shown in Fig. 9. The models of subunits Asa2, Asa4 and Asa7 were generated independently and then protein–protein docking predictions were carried out. The model that predicted an interaction between the carboxy-terminal half of Asa4 and the carboxy-terminal half of Asa7 was selected. Then, the model of the Asa2 subunit was docked on this subcomplex. The resulting model is shown in Fig. 9A. This model was then fitted on the 3D-model of the dimeric *Polytomella* ATP synthase generated by EM analysis (Fig. 9B) [7].

4. Discussion

The Asa subunits, which have been identified to date only in mitochondrial ATP synthases of chlorophycean algae, seem to be unique to this lineage [13]. As judged by single particle electron microscopy studies, the Asa subunits form a robust, peripheral stalk in the ATP synthase of *Polytomella* sp. that allows the enzymatic complex to function as a rotary motor [6]. Nevertheless, a more detailed picture of how these subunits interact was lacking. Here, we addressed the study of protein–protein interactions using the isolated, recombinant proteins of Asa2, Asa4 and Asa7 as well as some recombinant protein fragments, including the N-terminal and C-terminal halves of Asa4 (Asa4-N and Asa4-C respectively), as well as the corresponding fragments of Asa7 (Asa7-N and Asa7-C). The data obtained suggests that Asa2, Asa4 and Asa7 interact, and that there is a special strong interaction of Asa4 with Asa7, probably mediated by the C-terminal halves of both proteins. In addition, the data indicates that subunits Asa2, Asa4 and Asa7 may also

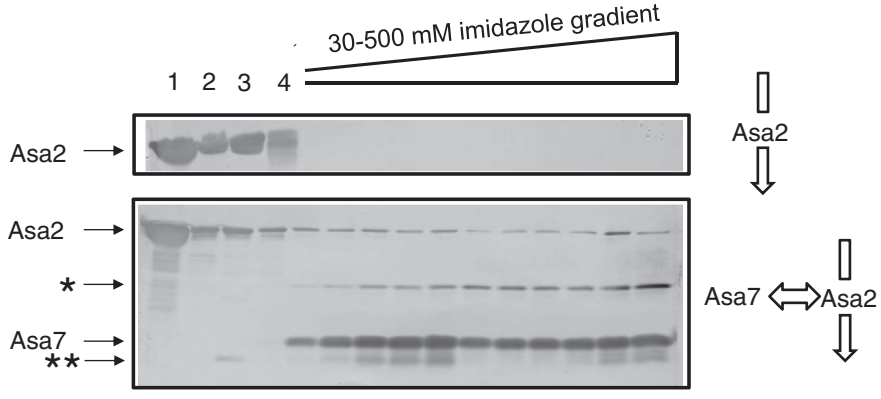

Fig. 6. The interaction of Asa2 with Asa7. A) Interaction of Asa2 and Asa7 assayed by affinity chromatography. The crude extract containing the recombinant Asa2 subunit was loaded on a 1 mL HisTrap column containing no bound protein (upper panel) or to which Asa7, containing a 6His-tag, was bound (lower panel). Western blot decorated with an anti-Asa2 and an anti-Asa7 antibody of the column fractions collected upon application of a 30–500 mM imidazole gradient. Lane 1, crude extract loaded on the column; lane 2, protein excluded from the column; lanes 3 and 4, proteins excluded from the column after washing with 30 mM imidazole.

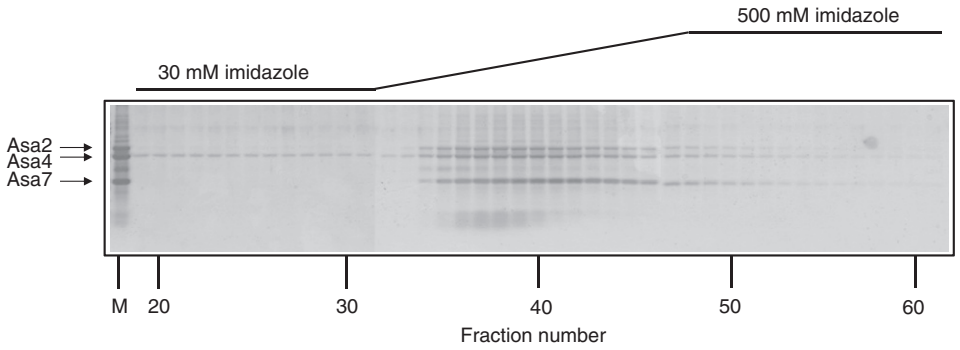

Fig. 7. Formation of an Asa2/Asa4/Asa7 subcomplex. The recombinant, isolated Asa2 (untagged), Asa4 (untagged) and Asa7 (6His-tagged) proteins form a stable subcomplex that can be recovered after affinity chromatography. The generated Asa2/Asa4/Asa7 subcomplex elutes when a linear imidazole gradient (30 to 500 mM) is applied. Lane M shows a mixture of the three recombinant proteins. Lanes 19 to 61 show the polypeptide composition of the 1 mL fractions collected from the column after washing with 30 mM imidazole (lanes 19 to 31); after applying the linear imidazole gradient (lanes 32–47); and after washing with 500 mM imidazole (lanes 31 to 61).

interact with Asa1 and with OSCP, suggesting their participation as structural components of the peripheral stalk. Also, we show that Asa2 may interact with an α subunit, and thus must be in close proximity to the F_1 sector. In addition, a mixture of Asa2, Asa4 and Asa7 seems to form a subcomplex in a 1:1:1 stoichiometry.

All the Asa subunits studied here were isolated in a denatured form and then solubilized and renatured. These renatured polypeptides clearly exhibited specific interactions, indicating that they did refold – either partially or fully – into their native conformations. In addition, circular dichroism spectral analysis of Asa2, Asa4, Asa4-N and Asa4-C indicated the presence of secondary structure in these polypeptides (data not shown).

RNA-mediated expression silencing of the Asa7 subunit in the green algae *C. reinhardtii*, a close relative of *Polytomella* sp., showed that the absence of this polypeptide neither affected growth nor the oxidative-phosphorylation properties of the alga [13]. Nevertheless, the intact, dimeric ATP synthase could not be purified from the Asa7-silenced mutant, because the complex invariably dissociated, releasing the F_1 sector. Therefore, Asa7 seems to be instrumental in stabilizing the peripheral stalk of the mitochondrial ATP synthase of chlorophycean algae. As suggested by the results obtained in this work, Asa7 interacts both with Asa2 and Asa4, and thus could be important in maintaining these subunits together, and thus helping stabilize the architecture of the peripheral stalk [7,10,11]. When heat dissociation of the intact ATP synthase of *Polytomella* sp. was followed in a time course, it was observed that several subunits, including Asa2, Asa4 and Asa7, readily dissociate from the complex [10]. Thus, these subunits seem to be in close contact in a region of the peripheral stalk that is highly susceptible to dissociation. We hypothesize that these three subunits are important architectural elements of the robust peripheral stalks of the algal enzyme as observed in EM. Subunit Asa1, although not addressed in this study, may be an important additional constituent of this stalk.

The model of the subcomplex Asa2/Asa4/Asa7 was fitted on the 3D model of the *Polytomella* mitochondrial ATP synthase complex obtained by a previous EM reconstruction [7]. Three considerations were taken into account to fit the subcomplex in this region of the peripheral stalk: *i*) the hydrophilic character of the Asa2, Asa4 and Asa7 subunits, which must be placed in a region relatively far away from the membrane region; *ii*) the proposed proximity of Asa2 to OSCP [7]; and *iii*) the proximity of Asa2 to subunit α. The model partially explains the important electron density of the peripheral stalks observed in the algal enzyme by EM. Nevertheless, these kinds of models have inherent limitations due to the multiple assumptions made at various steps of its in silico development: the 3D-modeling of polypeptides with all its variants, the modeling of their possible interactions by protein–protein docking, and the fitting of the generated subcomplex into the 3D structure derived from EM studies. It is therefore feasible that the Asa subunits may interact more closely with each other through helix–helix contacts, as the other constituents of the peripheral stalks of several eukaryotic [32–34], bacterial [35–37], and archaeal enzymes [38]. Prediction of coiled-coil segments [39] of the Asa subunits indicates a high propensity

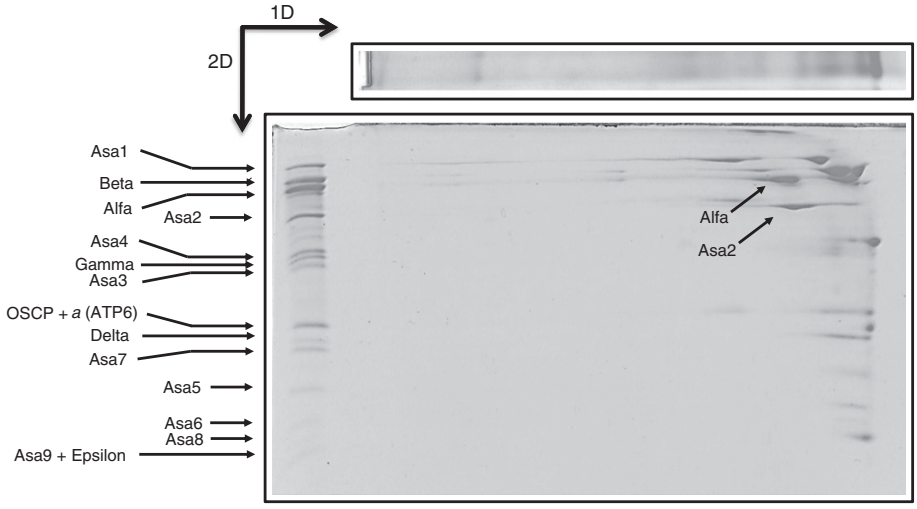

Fig. 8. An Asa2-alfa subunit subcomplex of the algal ATP synthase is generated by LiDS treatment. The purified algal ATP synthase (120 μg of protein) was incubated for 30 min on ice in the presence of 0.04% LiDS and then resolved by BN-PAGE in a 1D gradient gel of 4–12% acrylamide. The 1D gel was then subjected to 2D Tricine-SDS-PAGE (14% acrylamide) and stained with Coomassie Brilliant Blue. Fifty micrograms of purified algal ATP synthase was added as a control (lane C). The name of each subunit of the complex is indicated.

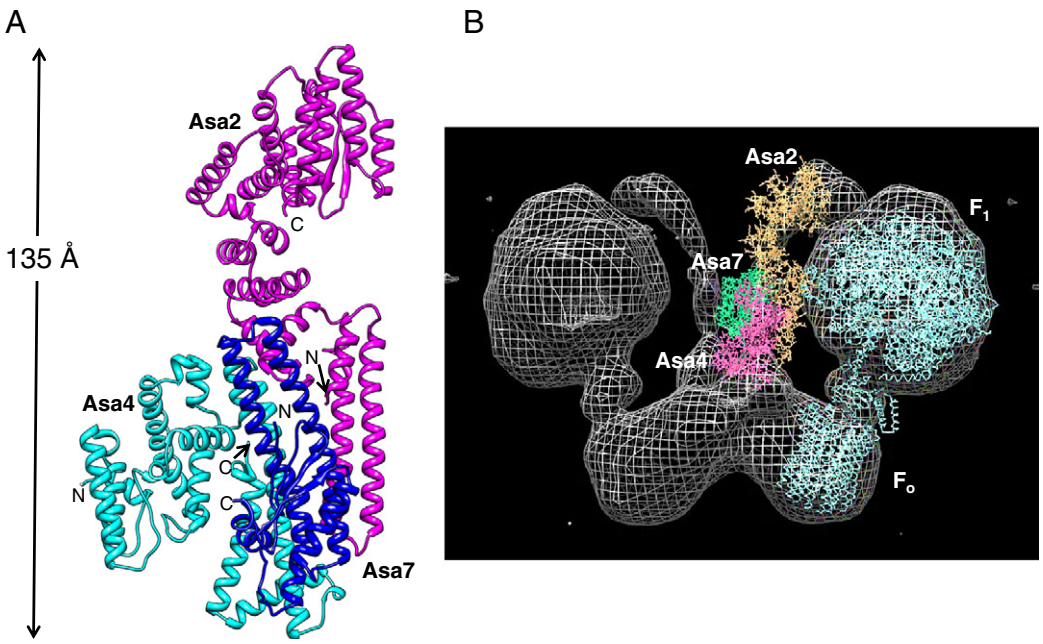

Fig. 9. Model of the Asa2/Asa4/Asa7 subcomplex. A) Model of the in silico generated Asa2/Asa4/Asa7 subcomplex. Subunit Asa2 is colored in magenta, Asa4 in cyan, and Asa7 in blue. The N- and C-termini are indicated with letters N and C, respectively. B) The Asa2/Asa4/Asa7 subcomplex was fitted in the previously generated 3D structure derived from EM studies. Subunits Asa2 (orange), Asa7 (green), Asa4 (pink) and the F_1 and Fo sectors (cyan) are indicated.

of some of these proteins to form this structural motif (30% of coiled-coil regions predicted for Asa1, 19% for Asa2, 35% for Asa4, and 32% for Asa7). Thus, these Asa subunits may intertwine in several regions to give rise to the stout peripheral arms that have been observed in *Polytomella* ATP synthase examined both by single-particle analysis [5–7] and dual-axis cryo-electron tomography [8].

The main function of the peripheral stalk is to hold the F_1 sector against the movement of the rotor stalk [40]. In the last years, it has become increasingly clear that this function may be achieved with peripheral stalks exhibiting different structures. For example, the peripheral stalk of bacteria is composed of two identical b subunits that extend as coiled-coil α helices from the bilayer to the delta subunit in the F_1 sector [41]. In contrast, the A-type ATP synthases of Archaea are structurally more closely related to vacuolar ATPases and exhibit two peripheral stalks composed by subunits E, H, and *a*. The two lateral stalks connect through a collar that surrounds the central stalk at a level above the A_0 sector and run upwards up to prominent knobs on the A_1 sector [42]. In eukaryotes like yeast, the peripheral stalk is composed of subunits b, d and h (also known as F6 in the bovine enzyme). The primary structure of the eukaryotic subunit b differs from the bacterial one, although it also extends as an alpha-helix, from the membrane region up to OSCP in the F_1 sector [43]. In contrast, other eukaryotic ATP synthases exhibit a polypeptide composition very different from the ones present in classical systems as yeast or bovine, especially in the region of the peripheral stalk. Such is the case of the ATP synthase of *Tetrahymena thermophila*, that exhibits a dramatically different architecture as observed by single particle electron microscopy projections and that contains at least 13 novel subunits apparently limited to the ciliate lineage [44]. Remarkably, besides lacking subunit *b*, this enzyme also lacks a classical subunit *a*. Nevertheless, a particularly robust peripheral arm is not observed in the ciliate enzyme. The additional protein mass seems to be distributed towards the membrane-embedded region and exposed to the mitochondrial intermembrane space. Proteomic analysis of *Trypanosoma brucei* has suggested that its ATP synthase is also highly divergent and exhibits 14 subunits which show no similarity to proteins outside the kinetoplastid lineage [45].

The presence of such robust peripheral stalks in the ATP synthase of chlorophycean algae raises questions about its flexibility. It has been argued that the peripheral stalk may store transient elastic energy during the rotary motion of the enzyme, functioning as an elastic buffer [46,47]. We speculate that a stout peripheral stalk as the one of *Polytomella* ATP synthase will have more than the necessary stiffness to counteract rotation of the central stalk, but will make less twisting motions, and thus will store less transient elastic energy.

Supplementary data to this article can be found online at http://dx.doi.org/10.1016/j.bbabio.2013.08.001.

Acknowledgements

We thank Laura Ongay Larios, Minerva Mora Cabrera and Guadalupe Códiz Huerta of the Molecular Biology Unit, IFC, UNAM for primer synthesis and sequencing. This research was supported by the grant 146044 from the Consejo Nacional de Ciencia y Tecnología (CONACyT) and Le Fonds National de la Recherche Scientifique (FNRS) exchange program B330/123/11 (Mexico–Belgium). Additional support was received from grants 128110 (CONACyT, Mexico), IN203311-3 from the Dirección General de Asuntos del Personal Académico (DGAPA-UNAM, Mexico) and from the Belgian F.R.S.-FNRS (MIS F.4520, FRFC 2.4597). CONACyT also supported with fellowships 229474 and 214946 the Ph.D. studies of H.M.-A. (Biomedical Sciences Ph.D. program at UNAM) and A.C.-E. (Biochemical Sciences Ph.D. program at UNAM) respectively. L.D.-R. thanks the PEW Charitable Trust for his postdoctoral fellowship.

References

[1] R.J. Devenish, M. Prescott, A.J. Rodgers, The structure and function of mitochondrial F1F0-ATP synthases, Int. Rev. Cell Mol. Biol. 267 (2008) 1–58.
[2] H. Seelert, N.A. Dencher, ATP synthase superassemblies in animals and plants: two or more are better, Biochim. Biophys. Acta 1807 (2011) 1185–1197.
[3] W. Junge, H. Sielaff, S. Engelbrecht, Torque generation and elastic power transmission in the rotary F(O)F(1)-ATPase, Nature 459 (2009) 364–370.
[4] R. van Lis, A. Atteia, G. Mendoza-Hernández, D. González-Halphen, Identification of novel mitochondrial protein components of *Chlamydomonas reinhardtii*. A proteomic approach, Plant Physiol. 132 (2003) 318–330.
[5] N.V. Dudkina, J. Heinemeyer, W. Keegstra, E.J. Boekema, H.P. Braun, Structure of dimeric ATP synthase from mitochondria: an angular association of monomers induces the strong curvature of the inner membrane, FEBS Lett. 579 (2005) 5769–5772.

[6] N.V. Dudkina, S. Sunderhaus, H.P. Braun, E.J. Boekema, Characterization of dimeric ATP synthase and cristae membrane ultrastructure from *Saccharomyces* and *Polytomella* mitochondria, FEBS Lett. 580 (2006) 3427–3432.
[7] A. Cano-Estrada, M. Vázquez-Acevedo, A. Villavicencio-Queijeiro, F. Figueroa-Martínez, H. Miranda-Astudillo, Y. Cordeiro, J.A. Mignaco, D. Foguel, P. Cardol, M. Lapaille, C. Remacle, S. Wilkens, D. González-Halphen, Subunit–subunit interactions and overall topology of the dimeric mitochondrial ATP synthase of *Polytomella* sp, Biochim. Biophys. Acta 1797 (2010) 1439–1448.
[8] N.V. Dudkina, G.T. Oostergetel, D. Lewejohann, H.P. Braun, E.J. Boekema, Row-like organization of ATP synthase in intact mitochondria determined by cryo-electron tomography, Biochim. Biophys. Acta 1797 (2010) 272–277.
[9] A. Atteia, G. Dreyfus, D. González-Halphen, Characterization of the alpha and beta-subunits of the F0F1-ATPase from the alga *Polytomella* spp., a colorless relative of *Chlamydomonas reinhardtii*, Biochim. Biophys. Acta 1320 (1997) 275–284.
[10] M. Vázquez-Acevedo, P. Cardol, A. Cano-Estrada, M. Lapaille, C. Remacle, D. González-Halphen, The mitochondrial ATP synthase of chlorophycean algae contains eight subunits of unknown origin involved in the formation of an atypical stator-stalk and in the dimerization of the complex, J. Bioenerg. Biomembr. 38 (2006) 271–282.
[11] R. van Lis, G. Mendoza-Hernández, G. Groth, A. Atteia, New insights into the unique structure of the F0F1-ATP synthase from the chlamydomonad algae *Polytomella* sp. and *Chlamydomonas reinhardtii*, Plant Physiol. 144 (2007) 1190–1199.
[12] A. Villavicencio-Queijeiro, M. Vázquez-Acevedo, A. Cano-Estrada, M. Zarco-Zavala, M. Tuena de Gómez, J.A. Mignaco, M.M. Freire, H.M. Scofano, D. Foguel, P. Cardol, C. Remacle, D. González-Halphen, The fully-active and structurally-stable form of the mitochondrial ATP synthase of *Polytomella* sp. is dimeric, J. Bioenerg. Biomembr. 41 (2009) 1–13.
[13] M. Lapaille, A. Escobar-Ramírez, H. Degand, D. Baurain, E. Rodríguez-Salinas, N. Coosemans, M. Boutry, D. Gonzalez-Halphen, C. Remacle, P. Cardol, Atypical subunit composition of the chlorophycean mitochondrial F_1F_O-ATP synthase and role of Asa7 protein in stability and oligomycin resistance of the enzyme, Mol. Biol. Evol. 27 (2010) 1630–1644.
[14] S. Funes, E. Davidson, M.G. Claros, R. van Lis, X. Pérez-Martínez, M. Vázquez-Acevedo, M.P. King, D. González-Halphen, The typically mitochondrial DNA-encoded ATP6 subunit of the F1F0-ATPase is encoded by a nuclear gene in *Chlamydomonas reinhardtii*, J. Biol. Chem. 277 (2002) 6051–6058.
[15] P. Cardol, D. González-Halphen, A. Reyes-Prieto, D. Baurain, R.F. Matagne, C. Remacle, The mitochondrial oxidative phosphorylation proteome of *Chlamydomonas reinhardtii* deduced from the Genome Sequencing Project, Plant Physiol. 137 (2005) 447–459.
[16] E.B. Gutiérrez-Cirlos, A. Antaramian, M. Vázquez-Acevedo, R. Coria, D. González-Halphen, A highly active ubiquinol–cytochrome c reductase (bc1 complex) from the colorless alga *Polytomella* spp., a close relative of *Chlamydomonas*. Characterization of the heme binding site of cytochrome c_1, J. Biol. Chem. 269 (1994) 9147–9154.
[17] X. Pérez-Martínez, M. Vázquez-Acevedo, E. Tolkunova, S. Funes, M.G. Claros, E. Davidson, M.P. King, D. González-Halphen, Unusual location of a mitochondrial gene. Subunit III of cytochrome C oxidase is encoded in the nucleus of chlamydomonad algae, J. Biol. Chem. 275 (2000) 30144–30152.
[18] R. van Lis, D. González-Halphen, A. Atteia, Divergence of the mitochondrial electron transport chains from the green alga *Chlamydomonas reinhardtii* and its colorless close relative *Polytomella* sp, Biochim. Biophys. Acta 1708 (2005) 23–34.
[19] H. Schägger, Denaturing electrophoretic techniques, in: G. von Jagow, H. Schägger (Eds.), A Practical Guide to Membrane Protein Purification, Academic Press, San Diego, 1994, pp. 59–79.
[20] H. Schägger, Native gel electrophoresis, in: G. von Jagow, H. Schägger (Eds.), A Practical Guide to Membrane Protein Purification, Academic Press, San Diego, 1994, pp. 81–104.
[21] M.A.K. Markwell, S.M. Hass, L.L. Biber, N.E. Tolbert, A modification of the Lowry procedure to simplify protein determination in membrane and lipoprotein samples, Anal. Biochem. 87 (1978) 206–210.
[22] R.R. Burgess, Refolding solubilized inclusion body proteins, Methods Enzymol. 463 (2009) 259–282.
[23] H. Schägger, H. Aquila, G. Von Jagow, Coomassie blue-sodium dodecyl sulfate-polyacrylamide gel electrophoresis for direct visualization of polypeptides during electrophoresis, Anal. Biochem. 173 (1988) 201–205.
[24] H. Towbin, T. Staehelin, J. Gordon, Electrophoretic transfer of proteins from polyacrylamide gels to nitrocellulose sheets: procedure and some applications, Proc. Natl. Acad. Sci. U. S. A. 76 (1979) 4350–4354.
[25] D. González-Halphen, M.A. Lindorfer, R.A. Capaldi, Subunit arrangement in beef heart complex III, Biochemistry 27 (1988) 7021–7031.
[26] R.A. Hall, Studying protein–protein interactions via blot overlay or Far Western blot, Methods Mol. Biol. 261 (2004) 167–174.
[27] S. Raman, R. Vernon, J. Thompson, M. Tyka, R. Sadreyev, J. Pei, D. Kim, E. Kellogg, F. DiMaio, O. Lange, L. Kinch, W. Sheffler, B.H. Kim, R. Das, N.V. Grishin, D. Baker, Structure prediction for CASP8 with all-atom refinement using Rosetta, Proteins 77 (Suppl. 9) (2009) 89–99.
[28] Y. Zhang, I-TASSER server for protein 3D structure prediction, BMC Bioinforma. 9 (2008) 40.
[29] E.F. Pettersen, T.D. Goddard, C.C. Huang, G.S. Couch, D.M. Greenblatt, E.C. Meng, T.E. Ferrin, UCSF chimera—a visualization system for exploratory research and analysis, J. Comput. Chem. 25 (2004) 1605–1612.
[30] A. Tovchigrechko, I.A. Vakser, GRAMM-X public web server for protein–protein docking, Nucleic Acids Res. 34 (2006) W310–W314.
[31] A.C. Wallace, R.A. Laskowski, J.M. Thornton, LIGPLOT: a program to generate schematic diagrams of protein–ligand interactions, Protein Eng. 8 (1995) 127–134.
[32] V.K. Dickson, J.A. Silvester, I.M. Fearnley, A.G. Leslie, J.E. Walker, On the structure of the stator of the mitochondrial ATP synthase, EMBO J. 25 (2006) 2911–2918.
[33] A. Poetsch, R.J. Berzborn, J. Heberle, T.A. Link, N.A. Dencher, H. Seelert, Biophysics and bioinformatics reveal structural differences of the two peripheral stalk subunits in chloroplast ATP synthase, J. Biochem. 141 (2007) 411–420.
[34] A.K. Welch, C.J. Bostwick, B.D. Cain, Manipulations in the peripheral stalk of the *Saccharomyces cerevisiae* F1F0-ATP synthase, J. Biol. Chem. 286 (2011) 10155–10162.
[35] Y. Bi, J.C. Watts, P.K. Bamford, L.K. Briere, S.D. Dunn, Probing the functional tolerance of the b subunit of *Escherichia coli* ATP synthase for sequence manipulation through a chimera approach, Biochim. Biophys. Acta 1777 (2008) 583–591.
[36] S.B. Claggett, M. O'Neil Plancher, S.D. Dunn, B.D. Cain, The b subunits in the peripheral stalk of F1F0 ATP synthase preferentially adopt an offset relationship, J. Biol. Chem. 284 (2009) 16531–16540.
[37] R. Priya, G. Biukovic, S. Gayen, S. Vivekanandan, G. Grüber, Solution structure, determined by nuclear magnetic resonance, of the b30-82 domain of subunit b of *Escherichia coli* F_1F_O ATP synthase, J. Bacteriol. 191 (2009) 7538–7544.
[38] A.M. Balakrishna, C. Hunke, G. Grüber, The structure of subunit E of the *Pyrococcus horikoshii* OT3 A-ATP synthase gives insight into the elasticity of the peripheral stalk, J. Mol. Biol. 420 (2012) 155–163.
[39] P. Fariselli, D. Molinini, R. Casadio, A. Krogh, Prediction of structurally-determined coiled-coil domains with hidden Markov models, Lect. Notes Comput. Sci 4414 (2007) 292–302.
[40] J.E. Walker, V.K. Dickson, The peripheral stalk of the mitochondrial ATP synthase, Biochim. Biophys. Acta 1757 (2006) 286–296.
[41] D.T. McLachlin, S.D. Dunn, Disulfide linkage of the b and delta subunits does not affect the function of the *Escherichia coli* ATP synthase, Biochemistry 39 (2000) 3486–3490.
[42] J. Vonck, K.Y. Pisa, N. Morgner, B. Brutschy, V. Müller, Three-dimensional structure of A_1A_0 ATP synthase from the hyperthermophilic archaeon *Pyrococcus furiosus* by electron microscopy, J. Biol. Chem. 284 (2009) 10110–10119.
[43] D.M. Rees, A.G. Leslie, J.E. Walker, The structure of the membrane extrinsic region of bovine ATP synthase, Proc. Natl. Acad. Sci. U. S. A. 106 (2009) 21597–21601.
[44] N.P. Balabaskaran, N.V. Dudkina, L.A. Kane, J.E. van Eyk, E.J. Boekema, M.W. Mather, A.B. Vaidya, Highly divergent mitochondrial ATP synthase complexes in *Tetrahymena thermophila*, PLoS Biol. 8 (2010) e1000418.
[45] A. Zikova, A. Schnaufer, R.A. Dalley, A.K. Panigrahi, K.D. Stuart, The F(0)F(1)-ATP synthase complex contains novel subunits and is essential for procyclic *Trypanosoma brucei*, PLoS Pathog. 5 (2009) e1000436.
[46] A. Wächter, Y. Bi, S.D. Dunn, B.D. Cain, H. Sielaff, F. Wintermann, S. Engelbrecht, W. Junge, Two rotary motors in F-ATP synthase are elastically coupled by a flexible rotor and a stiff stator stalk, Proc. Natl. Acad. Sci. U. S. A. 108 (2011) 3924–3929.
[47] A.G. Stewart, L.K. Lee, M. Donohoe, J.J. Chaston, D. Stock, The dynamic stator stalk of rotary ATPases, Nat. Commun. 3 (2012) 687.